Graphene/ferroelectrics/graphene hybrid structure: Asymmetric doping of graphene layers

Dinh Loc Duong, Si Young Lee, Seong Kyu Kim, and Young Hee Lee

Citation: Applied Physics Letters **106**, 243104 (2015); doi: 10.1063/1.4922448
View online: http://dx.doi.org/10.1063/1.4922448
View Table of Contents: http://scitation.aip.org/content/aip/journal/apl/106/24?ver=pdfcov
Published by the AIP Publishing

Graphene/ferroelectrics/graphene hybrid structure: Asymmetric doping of graphene layers

Dinh Loc Duong,[1,a)] Si Young Lee,[1] Seong Kyu Kim,[2] and Young Hee Lee[1,3,b)]
[1]*IBS Center for Integrated Nanostructure Physics, Institute for Basic Science, Sungkyunkwan University, Suwon 440-746, South Korea*
[2]*Department of Chemistry, Sungkyunkwan University, Suwon 440-746, South Korea*
[3]*Department of Physics, Department of Energy Science, Sungkyunkwan University, Suwon 440-746, South Korea*

(Received 11 November 2014; accepted 1 June 2015; published online 16 June 2015)

We report graphene/ferroelectric/graphene hybrid structure to demonstrate an asymmetrical doping in two graphene layers, one side with electrons and another side with holes. Two ferroelectrics, a poly(vinylidenefluoride) (PVDF) and a hydrofluorinated graphene, were used to demonstrate the concept with density functional calculations, revealing the Fermi level shift of 0.35 and 0.75 eV, respectively. This concept was confirmed by Raman spectroscopy using graphene/poly(vinylidenefluoride-co-trifluoroethylene)(P(VDF-TrFE))/graphene hybrid, which can easily form β-phase close to our simulation model. G-band peak position was downshifted for electron doping and upshifted for hole doping. This hybrid structure opens an opportunity to study bilayer graphene system with a controllable thickness for a wide range of high carrier concentration. © *2015 AIP Publishing LLC*. [http://dx.doi.org/10.1063/1.4922448]

Interaction strength between opposite carriers on two layers separated by a thin insulator has drawn attention for both theorists and experimentalists.[1–9] One can study many physical phenomena such as electron-hole plasma, electron-hole liquid, Bose-Einstein condensation, excitonic insulator, or BCS-like condensation, which are controlled by tuning the carrier concentration and the exciton radius on the layers.[6] The condensation of excitons, a bound state of electron-hole pairs, is expected to be observed up to 3–4 K, several orders higher than atom gases, due to their small effective mass.[6]

A system with a low disorder concentration is required to avoid elimination of quantum states. In the past, quantum well structure with high carrier mobility (e.g., GaAs) was used as active layers.[1,9] Graphene, an atomically thin layer with Dirac cone in the band structure, has been recently drawing attention in this field.[10,11] One ambitious expectation is that the condensation of excitons occurs at room temperature due to the extremely small mass of electron and low defect density in graphene.[12] However, several theoretical reports show controversial results that the critical temperature is only a mK range due to the screening effect.[13] The AB-stacked bilayer graphene has demonstrated the condensation temperature around several Kelvins.[14,15]

Although controversies still exist from different theoretical reports,[12,13,16] several experiments were performed to realize this concept. A typical experimental set up is that two exfoliated graphene flakes are isolated by a thin insulator such as h-BN or Al_2O_3 prepared by atomic layer deposition.[17–19] Carrier concentrations in graphene layers were controlled by top and bottom gates. No condensation has been observed, but a strong interaction near the Dirac point of hole and electron puddles on two graphene layers has been proven to exist up to 200 K.[17] This hole-electron interaction was reduced with increasing carrier concentration by applying gate voltages. This may originate from the many body interaction of carriers and gate-induced electric field as well.[8]

In this report, we propose an alternative strategy to implement an asymmetrical doping of two graphene layers by inserting ferroelectric materials. This hybrid structure consists of two graphene layers isolated by a ferroelectric layer. The strong dipole moment across ferroelectric layer gives rise to the asymmetrical doping on graphene layers on both sides: One side graphene layer is n-doped, and another side graphene layer is p-doped. This concept is proposed by the density functional calculations for two ferroelectrics: a poly(vinylidenefluoride) (PVDF) and hydro-fluorinated graphene with a Fermi level shift of 0.35 and 0.75 eV, respectively. Because of the difficulty to prepare β-phase PVDF experimentally, we chose a slightly different poly(vinylidenefluoride-co-trifluoroethylene)(P(VDF-TrFE) instead of theoretically investigated PVDF to build graphene/(P(VDF-TrFE))/graphene hybrid structure and performed Raman spectroscopy to confirm the simulation results.

The electronic and atomic structures were calculated by using density functional calculations implemented in Dmol3 package.[20] The numerical atomic basis sets with double numerical plus polarization were used with a cutoff radius of 4 Å. The generalized gradient approximation (GGA) under Perdew-Burke-Ernzerhof functional was used.[21] We notice that GGA underestimates van der Waals interaction. Therefore, the charge transfer and doping effect in our calculated results are underestimated as well. For a system of graphene-PVDF-graphene (Gr-PVDF-Gr), a 4 × 4 super

a)Current address: Max Planck Institute for Solid State Research, Heisenbergstrasse 1, D-70569 Stuttgart, Germany.
b)Author to whom correspondence should be addressed. Electronic mail: leeyoung@skku.edu

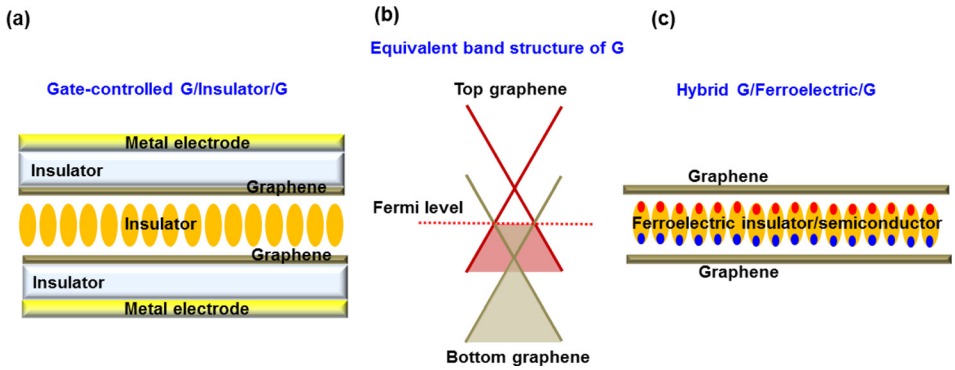

FIG. 1. Schematic of a configuration set up to obtain asymmetric doping between top and bottom graphene layers. (a) A common double-gate structure to control carrier concentration of two-layer system. (b) The equivalent band structure of graphene bilayer system. The top graphene layer is p-doped, while the bottom graphene layer is n-doped. (c) Graphene/ferroelectrics/graphene configuration.

cell of 32 carbon atoms was used. We applied the lattice constant of graphene for whole system that make 5% strain along PVDF chain.[22] A big vacuum of 30 Å was used along z-axis. $4 \times 4 \times 1$ k-point grid sampling by Monkhorst-Pack method was used for structural relaxation.[23] The structures were fully relaxed until the atomic forces on the atoms were smaller than 0.05 eV/Å. The dipole interaction between cells along z-direction was also corrected. The final results have been double-checked with VASP calculation. The projector augmented wave (PAW) potential was used with GGA-PBE functional and the same k-point mesh as Dmol3. A cut-off energy of 500 eV was used. The difference of results from VASP and Dmol3 was negligible. The charge transfer was calculated by Mulliken analysis method.[24]

Large-area monolayer graphene was grown by chemical vapor deposition on copper foil.[25] Monolayer graphene was transferred by a wet etching method using $FeCl_3$ and PMMA. A P(VDF-TrFE) (70:30) copolymer thin layer was prepared by Langmuir-Blodgett technique performed by a KSV Minitrough II.[26–28] A 0.01% solution of PVDF-TrFE in dimethyl sulfoxide (DMSO) was dropped on water surface. This solution of 1.2 ml was slowly dropped with a rate of 0.1 ml/minute. The surface pressure for the thin film transfer was 5 mN/m.[28]

In general, a two-gate structure is normally used to control the carrier on the top and bottom graphene, as shown in Fig. 1(a). The Fermi level of top and bottom graphene layer can be controlled by the top and bottom gate, respectively. Inverted symmetrical doping states can be formed, as shown in Fig. 1(b). Instead of this common configuration, we propose here an alternative structure using ferroelectric layer as an insulated layer. Ferroelectric layer has two opposite signs of charges: One F-terminated side is negative and another H-terminated side is positive, as shown in Fig. 1(c). This strong surface dipole moment located between two graphene layers introduces an asymmetrical doping effect on graphene: One layer is p-doped and another is n-doped.

To prove our concept, we built a representative model that consists of a PVDF layer placed between two graphene layers. The PVDF is a well-known ferroelectric material that can be arranged in a form of thin film with several hundred nanometers to a few nanometers.[26–28] Figure 2(a) shows the optimized configuration and induced charges formed by Gr/PVDF/Gr interaction. The optimized distance between two graphene layers is 9.04 Å. The induced charge is defined as $\rho_{\text{induced}} = \rho_{\text{total}} - \rho_{\text{graphene}} - \rho_{\text{PVDF}}$. The value of isosurfaces is $\pm 0.02\,\text{e/Å}^3$. Electrons on the bottom graphene layer are accumulated on graphene near the H-site of PVDF, while electrons at the top graphene layer are depleted on graphene near the F-site. The charge analysis shows that 0.17 e is accumulated on graphene near the H-site, while 0.18 e is depleted on graphene near the F-site. In contrast, a negligible amount of charges are accumulated on the PVDF (0.01 e). This phenomenon is understood by the large band gap of PVDF (about 6 eV, as shown in Fig. 3(a) by red color), which minimizes the electron transfer from PVDF to graphene. However, the local charge distribution on PVDF alters significantly. F atoms (the top part of PVDF) are more negatively charged, while H atoms (the bottom part of PVDF) are more positively charged. It implies that the surface dipole on PVDF increases when the PVDF is inserted between two graphene layers. We roughly estimated the dipole moment within an error of 6% of charge density. The dipole density is defined as $P = q\ d/A$, where q is charge on graphene layers, d is the distance between two graphene layers, and A is the area of the unit cell. The value of the dipole density is $0.52\ \text{D/Å}^2$.

A band structure of the hybrid system of Gr/PVDF/Gr is shown in Fig. 2(b). The Fermi level is set to zero and denoted as a red-dashed line. Two Dirac points are located at K-point above and below the red line. It simply indicates one graphene layer to be p-doped and another to be n-doped due to local charge distribution described above. The Fermi level is 0.35 eV downshifted in graphene near the F-sites and

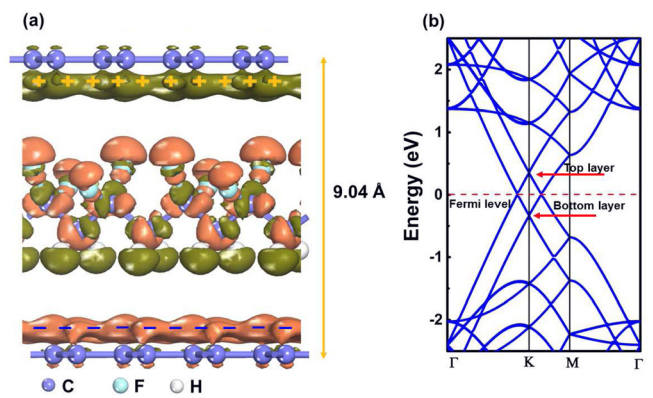

FIG. 2. The induced charge (a) and band structure (b) of a Graphene/PVDF/Graphene structure. The induced charge is defined as $\rho_{\text{induced}} = \rho_{\text{total}} - \rho_{\text{graphene}} - \rho_{\text{PVDF}}$. The value of isosurfaces is $\pm 0.02\ \text{e/Å}^3$. The brown and olive colors indicate the accumulation and depletion of electrons, respectively. The position of the Fermi level is taken as a reference.

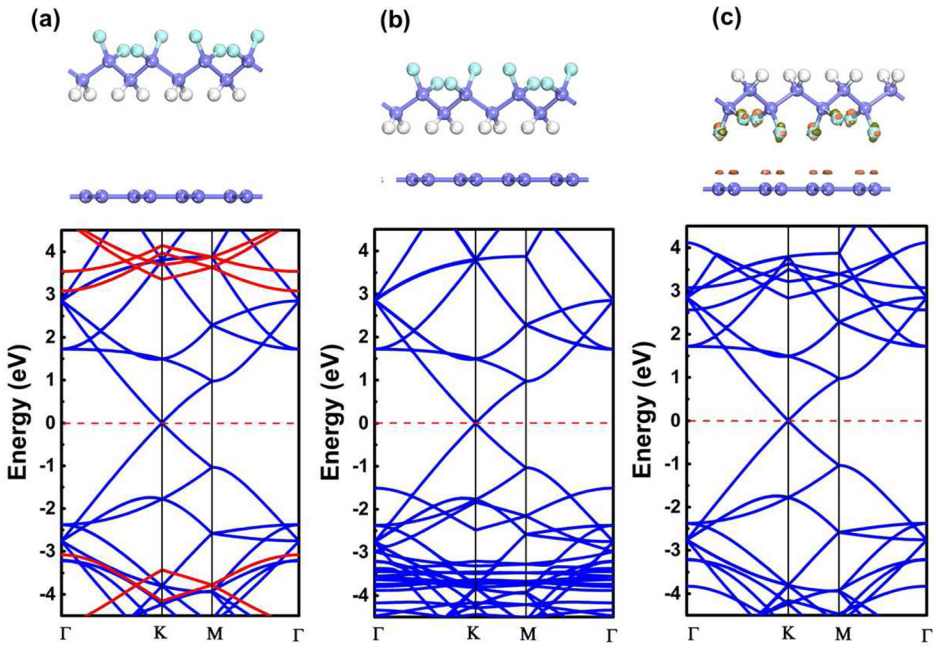

FIG. 3. The induced charge (top) and band structure (bottom) of a monolayer Graphene/PVDF structure: (a) separated graphene (blue) and PVDF (red), graphene and PVDF (b) with H-site contact, and (c) with F-site contact. The value of isosurfaces is $\pm 0.02\,e/Å^3$.

0.34 eV upshifted in graphene near the H-sites. The binding energy of PVDF with two graphene bilayers is 0.3 eV, equivalent to 0.37 eV/nm^2. This binding energy consists of top Gr layer-PVDF interaction, PVDF-bottom Gr layer interaction, and Coulomb interaction between electron on the top layer and hole on the bottom layer. Therefore, it is difficult to extract the electron-hole binding energy in general. In our approach, we calculated the binding energies of the top Gr-PVDF and PVDF-bottom Gr geometries separately. The binding energy of top Gr-PVDF and PVDF-bottom Gr are 0.12 eV and 0.09 eV, respectively. The energy gain with Gr-PVDF-Gr structure is 0.09 eV. This energy of 90 meV is defined as a binding energy between electron and hole.

To see the effect of PVDF in monolayer graphene, we performed band structure calculations. Figure 3(a) shows the band structure of PVDF and monolayer graphene when separated far away. The band gap of PVDF is around 6 eV with GGA calculations. Fermi level is located in the Dirac point of graphene. When PVDF attaches to graphene, a very small shift of Fermi level is observed in the calculated band structure, as shown in Figs. 3(b) and 3(c). This result is quite different with expectation of a strong doping effect to graphene from PVDF due to its strong dipole.[29–32] There are several reasons for this disagreement. GGA may underestimate van der Waals interaction that yields the small value of charge transfer. Another reason could be the difference in experiment and simulation configuration. In experiment, the ferroelectric layer is inserted between graphene and conducting layer (graphene, gold, electrolyte,…), which is similar to Gr-PVDF-Gr, while one side of graphene is in contact with vacuum in simulation configuration.[29–32] This suggests that the PVDF should be located between two conduction electrodes (graphene-PVDF-graphene or graphene-PVDF-metal) to get the doping effect to graphene. The band gap of ferroelectric layer may also affect the amount of charge transfers to graphene.[33,34] The amount of charge transfers are reduced with increasing the band gap of materials. We noticed that the band alignment of PVDF and graphene is strongly dependent on F-site or H-site. In the case of graphene near the H-site, the band structure of PVDF is downshifted, while it is upshifted in the case of graphene near the F-site.

To verify our proposal, we conducted an experiment to generate the hybrid structure. An ultrathin layer of P(VDF-TrFE) copolymer is used as a ferroelectric layer. This thin layer was formed by Langmuir-Blogett (LB) process on large-area monolayer graphene grown by chemical vapor deposition (CVD).[25,28] Figure 4(a) shows the partially deposited P(VDF-TrFE) layer (right part in the left panel) on graphene. AFM height profile is provided in the right panel to confirm the thickness of the film. The thickness of P(VDF-TrFE) is about 4 nm. The roughness of polymer is about 2 nm, higher than graphene roughness (below 1 nm). Figure 4(b) shows the uniformity of P(VDF-TrFE) film. The white dots in the left panel of Fig. 3(b) are PMMA residues after graphene transfer. Higher-resolution AFM image (right panel) shows several pinholes on the film. To check the asymmetrical doping effect on two graphene layers by ferroelectric layer, a structure of sandwiched three layers was fabricated. First layer is a monolayer graphene on SiO_2/Si, which was patterned by a photolithography. The second layer is a P(VDF-TrFE) layer deposited by the LB process. The third layer is another monolayer graphene, which was transferred onto the top of P(VDF-TrFE) layer. The Raman spectra are then measured at the position of monolayer and overlapped bilayer regions, as shown in Fig. 4(c). The G peak position of the top graphene layer at the monolayer region is 1593 cm^{-1} with a FWHM of 14 cm^{-1}, with a carrier density around 7×10^{12} cm^{-2}.[35] We observed that the G peak from overlapped region is more broadened than that from monolayer graphene. This peak was deconvoluted with Lorentzian shape into two smaller peaks because the signal is combined from two G peaks of top and bottom layers, 1584 cm^{-1} and 1593 cm^{-1} with 17 cm^{-1} and 14 cm^{-1} FWHM, respectively. This implies that the two graphene layers are doped at different doping level. We noticed that

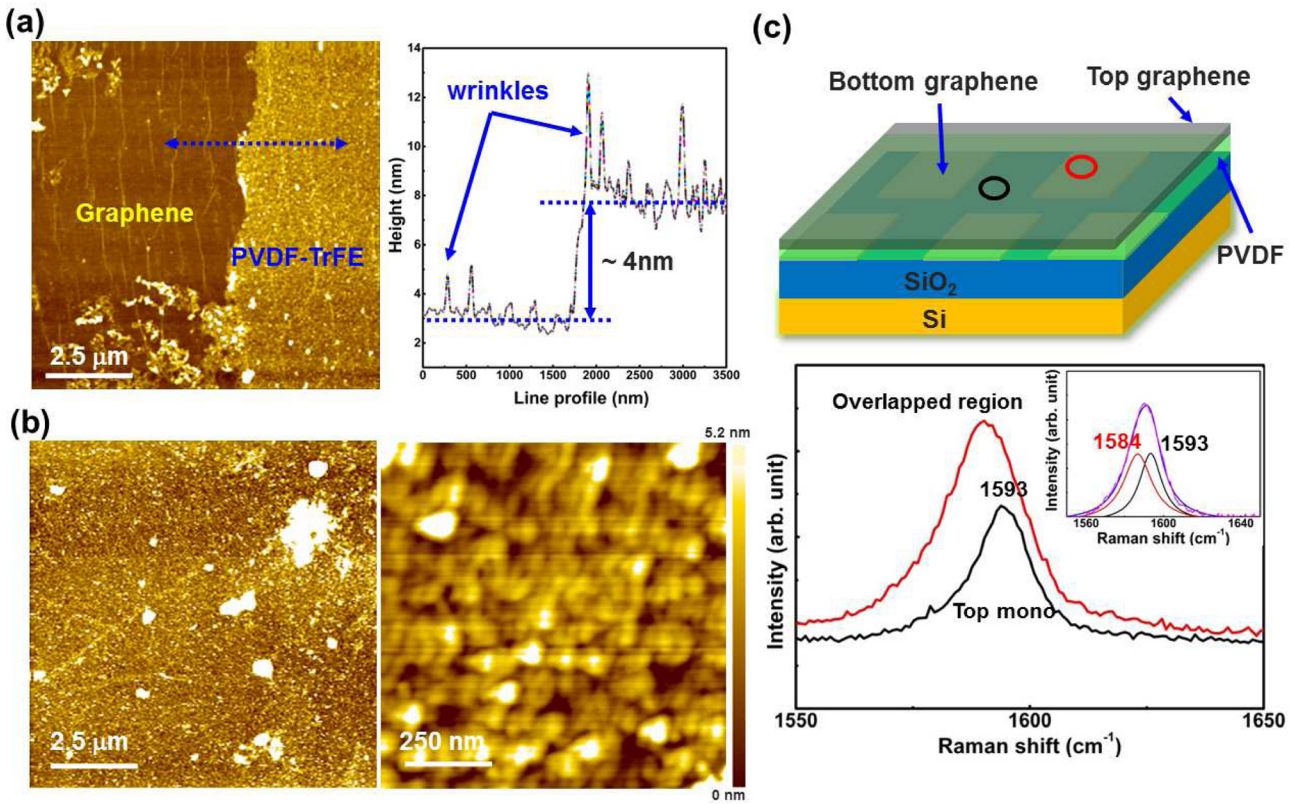

FIG. 4. (a) AFM morphology of graphene with P(VDF-TrFE) and thickness profile (right panel). (b) AFM morphology of P(VDF-TrFE) with 10 μm scan (left) and with 1 μm scan (right). (c) Schematic of Graphene/PVDF-TrFE/Graphene stacking device (top panel) and Raman spectra of graphene monolayer/bilayer region (bottom panel).

the variation of peak positions from position to position varied within 1 cm^{-1} in our samples. The initial graphene on SiO_2 before depositing P(VDF-TrFE) is 1587 cm^{-1}, intrinsically p-doped due to the transfer process or SiO_2/Si substrate effect. After forming the hybrid structure, the bottom graphene layer extracts electrons and compensates hole carriers eventually. The carrier concentration was reduced from 5×10^{12} to 2×10^{12} cm^{-2}. In contrast, the hole-doping in the top graphene layer is enhanced due to the loss of electrons. Therefore, the G-peak position is upshifted to 1593 cm^{-1}. This phenomenon is consistent with our theoretical simulation. It is of note that there was no poling process for P(VDF-TrFE) layer in our experiments. The initial p-type of the bottom graphene layer may lead to a self-assembly of P(VDF-TrFE) dipole moment.

Two-dimensional ferroelectric layer based on polymer has a drawback of pinholes as well as the lack of crystallinity at large area, making it difficult to get the uniformity of the aligned dipole in experiments. The Fermi level shift will therefore be smaller than simulation results. The thickness of the polymer is around 4 nm in experiments, four times larger than that of the calculated model. Therefore, an ideal 2D ferroelectric material is required if possible. Hydro-fluorinated graphene (HFG), a functionalized graphene with H atoms at one site and F atoms at another site, could be a good candidate, as shown in Fig. 5(a). This is a truly two-dimensional analog of polyvinylidene fluoride.[36] The optimized configuration and band structure of hybrid configuration of Gr/HFG/Gr are shown in Fig. 5. Two layers of graphene are asymmetrically doped. Top layer near the F-site of HFG is p-doped,

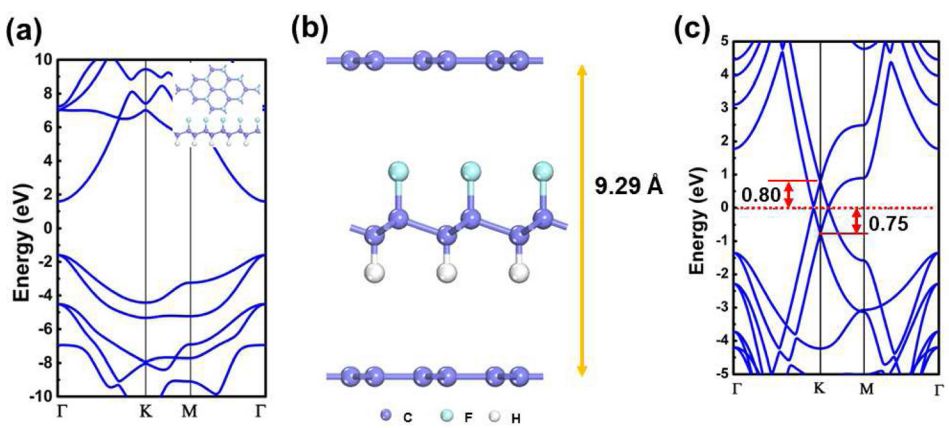

FIG. 5. (a) The band structure of hydro-fluorinated graphene (HFG). Inset is HFG configuration. (b) The optimized structure of Gr/HFG/Gr configuration. (c) Band structure of Gr/HFG/Gr. The Fermi energy is used as a reference.

whereas the bottom layer near the H-site of HFG is n-doped with a Fermi level shift of 0.80 eV and 0.75 eV, respectively. The charge analysis shows that 0.025 e is depleted on graphene near the F-site, while 0.024 e is accumulated on graphene near the H-site. The interlayer distance between two graphene layers is 9.25 Å. There is a band splitting from HFG structure at Gamma point due to small distortion of HFG structure by its interaction with graphene. The larger Fermi level shift in the case of HFG compared to PVDF is explained by stronger dipole moment per area and smaller band gap of HFG (about 2 eV) than that of PVDF (6 eV). Nevertheless, the similar effect generated from PVDF and HFG is a concrete evidence for generalization of our concept.

In summary, we proposed an alternative strategy of asymmetrical doping of two graphene layers sandwiched by ferroelectric materials. A ferroelectric material can be used as an asymmetrical doping agent for graphene, which can be used for both electronic applications and quantum state researches. The concept was demonstrated by both theoretical calculations and experiments. This doping strategy can be applied for not only graphene but also other 2D materials such as transition metal dichalcogenides. The hybrid structure of G/Ferroelectrics/G can be a good candidate for tunneling devices.

This work was supported by the Institute for Basic Science (IBS-R011-D1), Korea.

[1]U. Sivan, P. M. Solomon, and H. Shtrikman, Phys. Rev. Lett. **68**, 1196 (1992).
[2]L. V. Butov, A. C. Gossard, and D. S. Chemla, Nature **418**, 751 (2002).
[3]J. P. Eisenstein and A. H. Macdonald, Nature **432**, 691 (2004).
[4]J.-J. Su and A. H. MacDonald, Nat. Phys. **4**, 799 (2008).
[5]H. Deng, H. Haug, and Y. Yamamoto, Rev. Mod. Phys. **82**, 1489 (2010).
[6]L. V. Butov, MI Quantum Summer Sch. Progr., http://www.umich.edu/~mctp/SciPrgPgs/events/2010/M (2010).
[7]M. Richard, J. Kasprzak, A. Baas, S. Kundermann, K. G. Lagoudakis, M. Wouters, I. Carusotto, R. Andre, B. D. Pledran, and L. S. Dang, Int. J. Nanotechnol. **7**, 668 (2010).
[8]D. W. Snoke, Adv. Condens. Matter Phys. **2011**, 938609.
[9]D. Nandi, A. D. K. Finck, J. P. Eisenstein, L. N. Pfeiffer, and K. W. West, Nature **488**, 481 (2012).
[10]K. S. Novoselov, A. K. Geim, S. V. Morozov, D. Jiang, Y. Zhang, S. V. Dubonos, I. V. Grigorieva, and A. A. Firsov, Science **306**, 666 (2004).
[11]A. H. Castro Neto, N. M. R. Peres, K. S. Novoselov, and A. K. Geim, Rev. Mod. Phys. **81**, 109 (2009).
[12]H. Min, R. Bistritzer, J. J. Su, and A. H. MacDonald, Phys. Rev. B **78**, 121401 (2008).
[13]M. Kharitonov and K. Efetov, Phys. Rev. B **78**, 241401 (2008).
[14]D. Abergel, M. Rodriguez-Vega, E. Rossi, and S. Das Sarma, Phys. Rev. B **88**, 235402 (2013).
[15]A. Perali, D. Neilson, and A. R. Hamilton, Phys. Rev. Lett. **110**, 146803 (2013).
[16]M. Y. Kharitonov and K. B. Efetov, Semicond. Sci. Technol. **25**, 034004 (2010).
[17]R. V. Gorbachev, A. K. Geim, M. I. Katsnelson, K. S. Novoselov, T. Tudorovskiy, I. V. Grigorieva, A. H. MacDonald, S. V. Morozov, K. Watanabe, T. Taniguchi, and L. A. Ponomarenko, Nat. Phys. **8**, 896 (2012).
[18]S. Kim, I. Jo, D. C. Dillen, D. A. Ferrer, B. Fallahazad, Z. Yao, S. K. Banerjee, and E. Tutuc, Phys. Rev. Lett. **108**, 116404 (2012).
[19]S. Kim and E. Tutuc, Solid State Commun. **152**, 1283 (2012).
[20]B. Delley, J. Chem. Phys. **92**, 508 (1990).
[21]J. Perdew, K. Burke, and M. Ernzerhof, Phys. Rev. Lett. **77**, 3865 (1996).
[22]C. Duan, W. N. Mei, J. R. Hardy, S. Ducharme, J. Choi, and P. A. Dowben, Europhys. Lett. **61**, 81 (2003).
[23]H. Monkhorst and J. Pack, Phys. Rev. B **13**, 5188 (1976).
[24]R. S. Mulliken, J. Chem. Phys. **23**, 1833 (1955).
[25]D. L. Duong, G. H. Han, S. M. Lee, F. Gunes, E. S. Kim, S. T. Kim, H. Kim, Q. H. Ta, K. P. So, S. J. Yoon, S. J. Chae, Y. W. Jo, M. H. Park, S. H. Chae, S. C. Lim, J. Y. Choi, and Y. H. Lee, Nature **490**, 235 (2012).
[26]V. V. Arslanov, Russ. Chem. Rev. **63**, 1 (1994).
[27]S. Ducharme, Nature **391**, 874 (1998).
[28]L. M. Blinov, V. M. Fridkin, S. P. Palto, A. V. Bune, P. A. Dowben, and S. Ducharme, Usp. Fiziol. Nauk **170**, 247 (2000).
[29]M. Kalbac, J. Kong, and M. S. Dresselhaus, Phys. Status Solidi **250**, 2649 (2013).
[30]S.-H. Bae, O. Kahya, B. K. Sharma, J. Kwon, H. J. Cho, B. Özyilmaz, and J.-H. Ahn, ACS Nano **7**, 3130 (2013).
[31]Y. Zheng, G.-X. Ni, C.-T. Toh, C.-Y. Tan, K. Yao, and B. Özyilmaz, Phys. Rev. Lett. **105**, 166602 (2010).
[32]Y. Zheng, G.-X. Ni, S. Bae, C.-X. Cong, O. Kahya, C.-T. Toh, H. R. Kim, D. Im, T. Yu, J. H. Ahn, B. H. Hong, and B. Özyilmaz, Europhys. Lett. **93**, 17002 (2011).
[33]C. Baeumer, S. P. Rogers, R. Xu, L. W. Martin, and M. Shim, Nano Lett. **13**(4), 1693–1698 (2013).
[34]J. Ding, L.-W. Wen, H.-D. Li, X.-B. Kang, and J.-M. Zhang, Europhysics Lett. **104**, 17009 (2013).
[35]A. Das, S. Pisana, B. Chakraborty, S. Piscanec, S. K. Saha, U. V. Waghmare, K. S. Novoselov, H. R. Krishnamurthy, A. K. Geim, A. C. Ferrari, and A. K. Sood, Nat. Nanotechnol. **3**, 210 (2008).
[36]R. Singh and G. Bester, Phys. Rev. B **84**, 155427 (2011).